PCCP



PAPER

View Article Online



Cite this: Phys. Chem. Chem. Phys., 2020. 22. 4439

G4 accuracy at DFT cost: unlocking accurate redox potentials for organic molecules using systematic error cancellation†

Sarah Maier, Bishnu Thapa 🕩 and Krishnan Raghavachari 🕩 *

The redox potential is a powerful thermodynamic and kinetic tool used to predict numerous chemical and biochemical mechanisms. However, despite the improving predictive power of density functional theory (DFT), chemically accurate theoretical redox potentials are often difficult to achieve with DFT. For example, calculated redox potentials are sensitive to density functional choice and often fall short of the desired accuracy. Thus, ranges of errors for computed redox potentials between different density functionals can become guite large. The current study presents a cost-effective protocol that utilizes effective error cancellation schemes in order to accurately predict the redox potentials of a wide range of organic molecules. This computational protocol, called CBH-Redox, is an extension of the connectivity-based hierarchy (CBH) method, and produces thermochemical data with near-G4 accuracy. Herein, we test the CBH-Redox protocol against both experimental and G4 reference values and compare these results to DFT alone. Considering 46 C, O, N, F, Cl, and S atom-containing molecules, when using the CBH-Redox correction scheme, the MAEs for all eight density functionals tested are within the 0.09 V target accuracy versus both experiment and G4. Moreover, CBH-Redox achieves an impressive accuracy, with a MAE of 0.05 V or below when compared to G4 for six of the eight density functionals tested. In addition, when the CBH correction is applied, the error range across all functionals tested decreases from 0.12 V to about 0.05 V versus G4, and from 0.13 V to 0.04 V versus experiment.

Received 7th December 2019, Accepted 20th January 2020

DOI: 10.1039/c9cp06622e

rsc.li/pccp

Introduction

Predicting a system's tendency to undergo particular chemical transformations often requires a quantitative descriptor of the system's ability to gain or lose electrons. The redox potential, which describes the free energy cost of electron transfer, is one such descriptor. Indeed, the redox potential is a powerful thermodynamic and kinetic tool used to explain numerous chemical and biochemical mechanisms. For example, redox potentials control the binding activity and transcription mechanisms of DNA.¹⁻³ Redox properties play an important role in environmental chemistry, particularly in soil and sediment chemistry. 4,5 Additionally, redox potentials are widely studied in drug and catalytic design.^{6,7} Moreover, in recent decades, new developments in energy storage and redox flow batteries have stimulated new interest in redox properties and electrochemistry in general.^{8,9} Nonetheless, although such meaningful chemical descriptors are needed, achieving reliable and consistent

Department of Chemistry, Indiana University, Bloomington, Indiana 47405, USA. E-mail: kraghava@indiana.edu

† Electronic supplementary information (ESI) available: Redox potentials for all functionals tested along with mean absolute errors and corresponding tables and figures (XLSX); geometries (PDF). See DOI: 10.1039/c9cp06622e

redox potentials is a difficult task, both experimentally and theoretically. 10-12 Indeed, measured redox potentials are quite sensitive to any change in experimental setup. 12 In addition, redox potentials calculated using typical quantum chemistry packages are extremely sensitive to the chosen theoretical method. 10,11,13,14 Therefore, designing methods to produce highly accurate, reproducible redox potentials remains an outstanding task for scientists.

Experimental reduction potentials are usually obtained through techniques like cyclic voltammetry and pulse radiolysis. 15,16 In practice, experimental setups are highly sensitive to the choice of solvent, electrolytes, and reference electrode. 17-21 Moreover, the instability of certain radical organic reagents and the irreversibility of particular redox reactions make experimental measurements problematic. 17,22 Thus, while obtaining quantitatively accurate experimental measurements of redox potentials would prove invaluable, such experiments often encounter problems when it comes to accuracy and reproducibility. Thus, well-designed theoretical techniques provide a promising alternative in cases where consistent experimental measurements prove either problematic or impossible.10

Since their inception, quantum calculations have given chemists predictive power when it comes to determining which

chemical pathways are thermodynamically or kinetically favorable. Such methods, combined with accurate continuum solvent models, make theoretical predictions of redox properties possible. 10 Presently, several protocols exist for the theoretical determination of reduction potentials using continuum solvation models.¹⁰ The most common protocols involve calculating reduction potentials via a thermodynamic cycle, where the gas phase geometries of both species in a redox couple are then used to calculate free energies of solvation. 10,19,23-26 By contrast, some more recent protocols call for the direct computation of solution phase geometries and frequencies. Indeed, a recent study by Ho shows that direct calculation of solution phase geometries using the SMD solvent model gives reliable and accurate results when it comes to calculating redox potentials.²⁷ Both protocols described above commonly involve the use of semi-empirical or DFT methods due to the steep computational scaling of more accurate methods such as coupled cluster theory or the composite methods.^{28,29} Although the abovementioned protocols have helped greatly in the advancement of redox chemistry, they still fall short. Indeed, semi-empirical methods do not always give the desired accuracy, and DFT methods are sensitive to functional choice and often fall short due to the presence of systematic errors. 19,30,31 For these reasons, ranges of errors for redox potentials can become quite large. To illustrate, previous studies have reported errors between theory and experiment in the range of 100-500 mV. 11,23,26 Additionally, errors between quantum mechanical methods can range from tens to hundreds of milivolts.³² Therefore, a reliable and comprehensive protocol that eliminates systematic error in theoretical methods, without

Herein, a computational protocol for determining accurate redox potentials, based on systematic error cancellation techniques, generalized from the isodesmic schemes of Pople and co-workers, is presented.33 This protocol, called CBH-Redox, is an extension of the connectivity-based hierarchy (CBH) method previously introduced by Raghavachari and co-workers.³⁴ The CBH protocol was originally introduced as a method to calculate accurate thermodynamic properties of a wide range of organic molecules to within an error range of 2 kcal mol⁻¹. Since then, CBH has been used to predict thermochemical data for medium to large sized biomolecules and has also been extended to treat radicals and cations.35-37 CBH was recently used to predict the pK_a s for a data set of about 300 biomolecules to within 0.5 pK_a units of the experimental values.³⁷ The present work applies the CBH-2 protocol to a set of 46 organic molecules (containing C, O, N, Cl, F, and S atoms) in aqueous solvent to achieve redox potentials close to chemical accuracy. Additionally, the redox potentials of several sulfur-containing molecules were also computed in acetonitrile.

greatly increasing computational cost, would have striking value.

Computational redox potentials

The absolute reduction potential associated with the redox process shown below

$$Ox + e^- \leftrightarrow Red$$
 (1)

is generally calculated using the change in Gibbs free energy that occurs when a species either loses or gains an electron, and is given by the following expression:

$$E^{\circ} = \frac{-\Delta G_{\text{soln}}^*}{nF} \tag{2}$$

where F is Faraday's constant, $\Delta G^*_{\rm soln}$ is the change in Gibbs free energy associated with the reaction in solution, and n is the number of electrons being exchanged in the reaction.³⁸ Note that the charge on the oxidized (Ox) and reduced (Red) species is not indicated in eqn (1).

In order to compare redox calculations with experiment, a relative potential is computed. In this case, the potential is reported relative to an experimentally determined reference electrode potential:

$$E_{\rm rel} = E^{\circ} - E_{\rm ref} \tag{3}$$

where $E_{\rm rel}$ is the relative potential and $E_{\rm ref}$ is the potential of the reference electrode.³⁸

Therefore, the reliability of the relative redox potential is dependent on the accuracy of the experimentally measured reference potential. Unfortunately, reference values can vary significantly depending upon conditions of the measurements. For example, the experimental reference value for the standard hydrogen electrode (SHE) is usually reported within a relatively broad interval of 4.24-4.44 V.10 In addition, the reference value for the Fc/Fc⁺ couple can range from 0.4 to 0.64 V (versus SHE). 39,40 In many cases, a particular choice of solvent, electrolytes, and to a lesser extent temperature, can complicate reproducibility and can shift measurements by tens to hundreds of millivolts. Moreover, when using an aqueous reference electrode for a nonaqueous system, the liquid junction potential between the two solutions may cause further issues. 41 Therefore, finding data compatible with the majority of the literature is crucial, and if one wishes to reproduce experimental data, care must be taken in choosing the correct reference value. In this work, the SHE is used as the reference, with $E_{SHE} = 4.28 \text{ V}$, consistent with the parameterization of the SMD solvation model. 10,38 The free energy of the electron was taken to be 0 kcal mol^{-1} .⁴²

Currently, several protocols exist for calculating standard redox potentials in solution. One of the most common protocols employs the Born–Haber cycle, where the Gibbs free energy of the redox reaction in solution $(\Delta G_{\mathrm{soln}}^{*,\mathrm{rxn}})$ is determined from the free energy change in the gas phase $(\Delta G_{\mathrm{gas}}^{*,\mathrm{rxn}})$ along with the solvation free energies of the oxidized and reduced species $(\Delta G_{\mathrm{solv}}^{\mathrm{Red/Ox}})^{10}$. A scheme for this thermodynamic cycle is shown in Fig. 1.

Although this is the most common route taken, recent work by Ho has shown that when using the SMD solvation model, the direct calculation of pK_as and reduction potentials in solution yields accurate results, with negligible differences in most cases, when compared to values calculated using a thermodynamic cycle. ^{27,43} More importantly, direct calculation of solution phase geometries and frequencies may also lend some improvement for larger molecules, such as amino acids, where conformational changes upon solvation may need to be taken into account. ²⁷

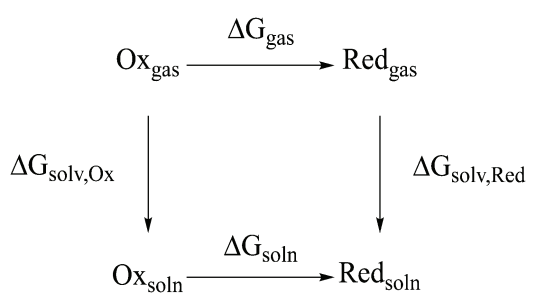


Fig. 1 Thermodynamic cycle for the determination of redox potentials.

Therefore, for this work, all geometry and frequency calculations were performed directly in solvent using the SMD implicit solvation model.

If the redox reaction is sensitive to pH, then hydrogen ions are transferred in the process and the redox reaction is often referred to as a proton-coupled electron transfer (PCET). In this case, the redox reaction is dependent on the pH of the system, and eqn (2) is altered to reflect this pH dependence.⁴⁴ The reduction potential for such a reaction is given by:

$$E_{\text{PCET}} = E^{\circ} - 0.059 \cdot \text{pH (at 25 °C)}$$
 (4)

In this study, the redox potentials of phenolic and tyrosine compounds were calculated using the PCET formalism. To check the likelihood of deprotonation, pK_a values were computed for these species using B3LYP/6-311++G(3df,2p) level of theory, and are reported in the Results section. Deprotonation for the rest of the species was deemed unfavorable. The pK_a is calculated through the following relationship:

$$pK_{a} = \frac{\Delta G_{deprot}^{*}}{2.303 \cdot RT}$$
 (5)

where $\Delta G^*_{\mathrm{deprot}}$ is the free energy change associated with deprotonation in solvent, R is the gas constant, and T is the temperature. 45 In the calculation of pK_a , the aqueous phase free energy of the proton is obtained through a thermodynamic cycle. $G_{\mathrm{H^{+},aq}}^{*}$ was set to -270.29 kcal mol⁻¹, which is the summation of $G^*_{\mathrm{H^+,solv}} = -265.9 \; \mathrm{kcal} \; \mathrm{mol}^{-1}$, $G^{\circ}_{\mathrm{H^+}} = -6.28 \; \mathrm{kcal} \; \mathrm{mol}^{-1}$, and $\Delta G_{\text{L}_{+}}^{\text{1 atm} \to 1 \text{ M}} = 1.89 \text{ kcal mol}^{-1}.^{46-48}$

Construction of the CBH-Redox protocol

The connectivity-based hierarchy (CBH) approach is a chemically intuitive, structure-based method to achieve highly accurate thermochemical calculations. 34 CBH provides a local correction to the electronic environment of molecular fragments using a connectivity-based generalization of the isodesmic, homodesmotic, and related schemes proposed by Pople, George, and many others. 31,33,49,50 The hierarchy of error cancelation schemes outlined in the CBH protocol is well defined, and a complete explanation of the CBH hierarchy and its rungs (CBH-0, CBH-1, CBH-2, etc.) can be found in the first of a series of CBH studies by Raghavachari and co-workers.³⁴ Essentially, when moving up

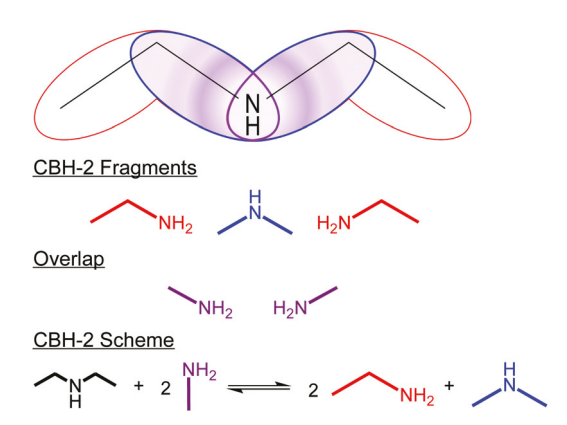


Fig. 2 Illustration of CBH-2 fragmentation scheme for diethylamine.

the rungs of the hierarchy, fragment size becomes larger, with CBH-0 prescribing fragments composed of only a single heavy atom, CBH-1 prescribing fragments consisting of two heavy atoms, and CBH-2 prescribing fragments consisting of one heavy atom along with those heavy atoms in its immediate bonding environment (Fig. 2).

Similar to the reaction schemes detailed by Wheeler, Houk, Schleyer, and Allen, CBH schemes exploit the intrinsic error cancellation of reactions that balance local bonding environments to improve the accuracy of quantum calculations.⁴⁹ According to the CBH protocol, the molecule is first calculated at a cheap or low level (LL) of theory, for example DFT. The molecule is then fragmented according to a particular rung in the hierarchy, and a CBH scheme for that molecule is made, taking fragment overlap into account. This scheme is then used to calculate a corrective term to be added to the energy of the low-level calculation.

Fig. 2 illustrates the CBH-2 scheme that is followed in this work, using diethylamine as an example. As mentioned earlier, in the CBH-2 fragmentation scheme, the immediate connectivity of all the atoms in the molecule is preserved, i.e., every heavy atom is extracted with its immediate bonding environment. After fragmentation is completed, the fragment energies are computed at both a low level (LL) of theory (e.g., DFT) and at a more sophisticated but expensive high level (HL) of theory (e.g., the Gaussian-4 composite method, G4). Proceeding further, the difference between the summed energies of the G4 fragments and the summed energies of the DFT fragments is then computed. It should be noted that each fragment preserves a portion of the total electronic environment, and the sum of the fragment energies should approximate the energy of the full molecule. Therefore, the correction to the DFT full energy is obtained by:

$$E_{\rm G4}({\rm full}) - E_{\rm DFT}({\rm full}) \approx \sum_{i} E_{\rm G4}(i) - \sum_{i} E_{\rm DFT}(i)$$
$$= \Delta {\rm CBH_{\rm corr}} \tag{6}$$

where E_{G4} (full) is the energy of the full molecule calculated with G4, E_{DFT} (full) is the energy of the full molecule calculated with DFT, $E_{G4}(i)$ is the energy of the *i*th fragment calculated with G4, $E_{\text{DFT}}(i)$ is the energy of the *i*th fragment calculated with DFT, and ΔCBH_{corr} is the total CBH correction to be applied to full

DFT energy. Thus, it is the difference of the summed fragment energies which provides a correction to the DFT energy of the full molecule.

When this correction is added to the full DFT energy, the full G4 energy is approximated as:

$$E_{\rm G4}({\rm full}) \approx E_{\rm DFT}({\rm full}) + \Delta {\rm CBH}_{\rm corr} = E_{\rm G4}^{\rm CBH}$$
 (7)

It is important to observe that the closer the fragments are in representing the local bonding environment in the full molecule, the better the CBH approximation becomes. Indeed, as one moves higher up on the hierarchy and fragment size becomes larger, CBH-corrected energies should improve. Therefore, larger fragments will in general produce more accurate CBH corrections.

Taking it one step further, the basic CBH protocol can be modified to compute accurate redox potentials. Using the same protocol outlined above, one can compute accurate Gibbs free energies. In particular, one may compute the Gibbs free energies associated with the redox couple in eqn (1) to obtain $\Delta G_{\text{soln}}^{*,\text{CBH}}$:

$$\Delta G_{\text{rxn,soln}}^{*,\text{CBH}} = G_{\text{Red,soln}}^{*,\text{CBH}} - G_{\text{Ox,soln}}^{*,\text{CBH}}$$
 (8)

From $\Delta G_{\rm rxn,soln}^{*,{\rm CBH}}$, one can subsequently obtain reduction potentials according to eqn (2) and (3). As an example, the CBH-Redox scheme for 3-(2-methoxyphenolxy)-1,2-propanediol is shown in Fig. 3 following the CBH-2 scheme for fragmentation. Once the CBH-2 scheme is determined, $\Delta G_{\rm soln}^{\rm CBH}$ can be computed accordingly (Fig. 4).

Notice that because calculating reduction potentials involves computing relative energies, many of the fragment energies of the reduced and oxidized species cancel with one another. Additionally, due to their small size, the computational cost for HL fragments is low. Notice also that in the case of the

Construction of hypohomodesmic reaction schemes

(Red)
$$_{HO}$$
 $_{OH}$ $_{OH}$

Fig. 3 CBH-2 fragmentation scheme for 3-(2-methoxyphenolxy)-1,2-propanediol redox couple.

$$\Delta G_{soln}(CBH) = \begin{bmatrix} (CBH_{corr}|Red) & (CBH_{corr}|Ox) \\ (CBH_{corr}|Ox) & (CBH_{corr}|Ox) \\ (CBH_{corr}|Ox) & (CBH_{corr}|Ox) \\ (CBH_{corr}|Ox) & (CBH_{corr}|Ox) & (CBH_{corr}|Ox) \\ (CBH_{corr}|Ox) & (CBH_{c$$

Fig. 4 Example of change in Gibbs free energy obtained from CBH-2 scheme.

fragments, only the electronic energies must be considered if both the HL and the LL fragments are optimized at the same level of theory. This fact is due to the cancellation of the thermal correction to the HL fragment by the corresponding thermal correction to the LL fragment. A brief outline of the full CBH-Redox protocol is given in Fig. 5.

CBH Scheme Setup

- 1. Select appropriate HL and LL.
- Construct CBH fragmentation scheme for redox pair.
- Determine net fragment reaction for correction.

Full Molecule

- Optimize and calculate frequencies and thermal correction to G.
- Using the optimized geometry from previous step, perform LL single point calculation
- Add thermal correction from 4 to the electronic energy (EE) from step 5.

Fragments

For both species in redox pair:

- 7. Optimize associated fragments and calculate frequencies and thermal correction to G.
- Using the optimized geometry from previous step, perform HL and LL single point calculations.
- 9. Add thermal correction from 7 to the EE from step 8. (If HL and LL optimization and frequencies are done at the same level of theory, then only EE of fragments are needed.)
- 10. Sum LL fragment energies-either G or EE, depending on step 9.
- 11. Sum HL fragment energies-either G or
- 12. Subtract (10) from (11). This is the CBH correction to G.

CBH Redox Potentials

- 13. Add CBH correction to G of the LL full molecule.
- 14. Using the CBH-corrected values of G for each species in the redox couple, compute the CBH-corrected ΔG.
- Compute CBH-corrected redox potential using values calculated in

Fig. 5 CBH-Redox protocol.

Electronic structure methods

All calculations were performed using the Gaussian 16 suite of programs.⁵¹ Eight density functionals were chosen to test the overall performance of the CBH-Redox protocol. These density functionals include: the popular hybrid functional B3LYP, Truhlar's meta-exchange-correlation functional M06-2X, the long-range corrected CAM-B3LYP functional, Head-Gordon's long-range corrected wB97X functional, and their dispersioncorrected counterparts, B3LYP-D3BJ, CAM-B3LYP-D3BJ, M06-2X-D3, and ωB97X-D, respectively. An unrestricted Kohn-Sham wavefunction was used for all radical species. 52-59

Optimizations of the full molecules and the fragments were performed at the B3LYP/6-31G(2df,p) level of theory to match the Gaussian-4 (G4) composite method, with frequencies of the full molecules being scaled by 0.9854.60-62 Optimization and frequency calculations for all species were performed directly in aqueous solvent using the SMD solvation model.43 It should be noted that frequency calculations were computed under standard state conditions of 1 mol L^{-1} at 298.15 K. All structures were verified to be local minima. Following optimization, single-point calculations of the full molecules as well as their fragment molecules were performed in solvent with one of the functionals listed earlier, along with the larger 6-311++G(3df,2p) basis set.⁶⁰⁻⁶² G4 theory, which typically reproduces thermochemical data to ~ 1 kcal mol⁻¹, was chosen as the high level of theory in the CBH-Redox protocol, and thus fragment energies were also calculated using G4 composite theory.²⁹

Due to the variability of experimental conditions, assembling a highly accurate set of experimental reference values compatible with the majority of the literature is a challenging task. Therefore, we elected to compare our calculated redox potentials to both experiment and to values calculated directly with the accurate G4 composite theory. Thus, serving to enhance the overall assessment of the protocol prescribed herein, G4 calculations were carried out in solvent for all full neutral, radical, and cationic species considered in this work.

Definition of test set and reference values

For the present study, a set of 46 organic molecules was chosen to demonstrate the scope and relevance of the CBH-Redox protocol (Fig. 6). The redox properties of organic molecules play a huge role in biochemical activity, drug design, and synthetic organic chemistry. Moreover, when compared to inorganic materials such as lithium, organic molecules are often cheaper and less toxic, and have therefore been suggested as promising electro-active candidates for flow batteries.9 The test set contains a variety of hetero atoms (e.g., C, N, O, F, S, Cl), a wide range of functional groups (e.g. acids, alcohols, aldehydes, alkyl-halides, amines, ethers, ketones, nitriles, nitro compounds, phenyls, thioethers), and varying degrees of linearity and conjugation. Additionally, tyrosine, whose reduction potential influences many biological mechanisms, including DNA synthesis and

43

44

ig. 6 Test set of phenols, anilines, methoxy benzene, amines, and amino acids

42

water oxidation, was included in the set as an interesting test case for the CBH-Redox protocol. 63 The experimental values were taken from cyclic voltammetry, square wave voltammetry, pulse radiolysis, or differential pulse polarography studies. 10,27,64-68 Moreover, all redox reactions involve only a single electron transfer. It is important to note also, that most molecules included in the test set are large enough that full G4 calculations are fairly costly, and thus are suitable candidates for the CBH-Redox protocol. Calculations for all 46 molecules were performed in aqueous solvent. However, in the case of the sulfur-containing compounds, redox calculations were also performed in acetonitrile for comparison. Thioethers are readily oxidized to sulfoxides and sulfones in aqueous solvent, often resulting in electrochemical irreversibility. Therefore, accurate experimental results for such species are difficult to achieve. Moreover, although cyclic voltammetry experiments of sulfides generally result in irreversible plots regardless of solvent, one need not consider the effects of acid-base chemistry when computing the potentials in acetonitrile. Thus, redox potential values in acetonitrile are a useful comparison, as some recent studies have shown that for some sulfide species such as methionine, the redox potential changes depending on the pH of the system.69

With the test set established, careful analysis of the reference data is needed in order to obtain a meaningful benchmark analysis of the CBH-Redox protocol. In order to mitigate the possible deficiencies in experimental reference values, G4 redox potentials are also used as a reference. Note that the present

work involves the reduction of radical-cation species; therefore, all data reported is based on calculations involving open shell species. Because this study employs only single determinant methods, spin contamination must be considered. While it has been shown that DFT suffers less from spin contamination, wavefunction methods are prone to greater contamination by higher spin states.^{70,71} All radical species considered in the present work are doublets and should have $\langle S^2 \rangle$ values of 0.75. However, at the wavefunction-based steps of the G4 calculation, nearly all radical species have significant spin contamination, with many $\langle S^2 \rangle$ values at the CCSD(T) step lying close to 1.2. The maximum $\langle S^2 \rangle$ value observed is about 1.8 before annihilation. By contrast, for all DFT methods, the radical $\langle S^2 \rangle$ values hover around 0.75, the largest values being less than 0.81. Moreover, the $\langle S^2 \rangle$ values of the G4 daughter fragments likewise hover closer to 0.75, with a maximum observed value of about 0.85. Unlike many of the parent molecules, which have a high degree of delocalization due to the presence of aromatic rings, the daughter fragments experience decreased spin contamination, possibly due to the loss of aromaticity and thus spin delocalization in the fragments. Indeed, the unrestricted wavefunction is likely to be more appropriate for the smaller systems where orbitals are less delocalized.

45

46

Thus, while the effects of spin contamination are rather minimal in the full LL calculations and in the fragment LL and HL calculations, further analysis of the full G4 reference values is required. Fig. 7 shows the correlation between 43 reference redox potentials (not including sulfur-containing compounds)

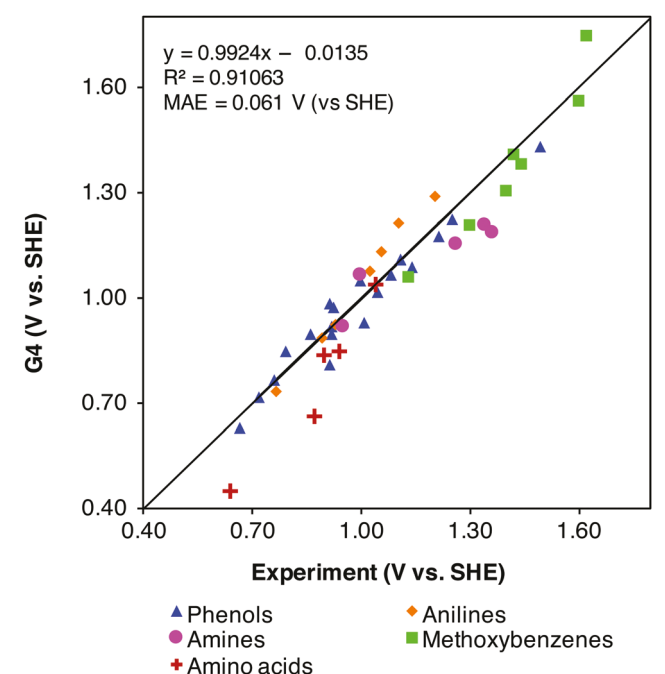


Fig. 7 Correlation between calculated G4 redox potentials and corresponding experimental values.

in aqueous solvent determined experimentally and those determined using G4. Here, G4 achieves a mean absolute error (MAE) of 0.06 V (vs. SHE), or about 1.4 kcal mol^{-1} , compared to experiment, and an R^2 value of 0.91. Thus, despite the deviations in $\langle S^2 \rangle$, this set of reference G4 potentials is still regarded as a valid complementary reference to experimental results. In the G4 calculation, CCSD(T) eliminates the S + 1contaminant and reduces the S + 2 contaminant.⁷¹ Moreover, CCSD(T) has been found to be somewhat insensitive to choice of unrestricted or restricted orbitals in predicting energies.⁷¹ Because the wavefunction-based steps following the CCSD(T) calculation in G4 are used for the addition of only corrective differences to the CCSD(T) energy, the effects of spin contamination in the G4 calculations may be partly cancelled, and thus may play only a small role in the overall energy.²⁹

Results and discussion

Using the CBH-Redox protocol, redox potentials for 46 organic molecules in aqueous solvent and several sulfur-containing compounds in acetonitrile were obtained using eight different density functionals. As in previous applications of CBH, the target accuracy for the present study was set to 2 kcal mol⁻¹ error, or about 0.09 V, when comparing with experimental and G4 values. 35-37,72 For CBH schemes involving radicals, it is important to note that in order to achieve effective error cancellation, radical location must be known with some certainty. If not, the radical may be placed on the incorrect fragment. Incorrect radical placement can lead to insufficient bond matching and poor error cancellation. For phenolic compounds and tyrosine derivatives,

the radical is placed on the fragment containing the aryl OH group, for the anilines the radical is placed on the fragment containing the aryl nitrogen, for the amines the radical is placed on the nitrogen containing fragments, and lastly for the methoxy benzenes, the radical is placed on the fragments containing the aryl methoxy group. Lastly, one may argue that although the fragments do not exactly replicate the Gibbs energies of a single species in a redox couple, accurate reaction Gibbs free energies can still be obtained if the energy difference between reduced and oxidized fragments is representative of the energy difference between the reduced and oxidized parent molecules. It should be noted that electron delocalization in the full molecule is captured at the low level of theory.

For the phenolic compounds as well as the tyrosine derivatives, a PCET formalism was used to compute the redox potentials. As evidence to suggest a PCET, in a 1975 study on the acidity constants of phenol radical cations in 0 to 75% sulfuric acid, the species considered were observed to have negative p K_a s.⁷³ In a more recent study, an estimate of -2.0 is given for the pK_a of the tyrosine radical cation, and the paper further suggests that tyrosine/phenol oxidation occurs via a concerted transfer of H⁺ + e⁻ in aqueous neutral solutions.⁷⁴ Indeed, due to their high reactivity, these radical cation species are difficult to isolate experimentally. Thus, we provide only the calculated pK_as for the phenol and tyrosine compounds in Table 1. The calculated pK_as of the radical cations in Table 1 also suggest the appropriateness of the PCET treatment for these molecules.

The MAEs for LL uncorrected and CBH-corrected redox potentials versus experiment are shown in Fig. 8 for 43 nonsulfur compounds, for each of the eight density functionals tested. Of the functionals tested, B3LYP, B3LYP-D3BI,

Table 1 pKa values for radical cation species calculated at B3LYP/ 6-311++G(3df,2p)

	pK _a	
(1) 2,6-Dimethoxyphenol	-5.5	
(2) 2-Methoxy-4-formylphenol	-12.7	
(3) 2-Methoxyphenol	-4.1	
(4) 3-Hydroxy-acetophenone	-8.5	
(5) 3-Methoxyphenol	-3.3	
(6) 4-Ethyl-2-methoxyphenol	-3.3	
(7) 4-Ethylphenol	-5.1	
(8) 4-Hydroxy-acetophenone	-9.1	
(9) 4-Methoxyphenol	-2.6	
(10) Bisphenol-A	-3.2	
(11) Triclosan	-8.2	
(12) 3-Chlorophenol	-8.7	
(13) 2,4,6-Trichlorophenol	-14.1	
(14) 2,4-Dinitrophenol	-14.9	
(15) 2,5-Dimethylphenol	-5.1	
(16) 2-Chlorophenol	-9.9	
(17) 2-Phenylphenol	-6.4	
(18) 4-Nitrophenol	-12.3	
(19) 4-Cyanophenol	-10.5	
(39) 3-Amino-L-tyrosine	-1.3	
(40) 3-Methoxy-L-tyrosine	-4.3	
(41) 3-Nitro-L-tyrosine	-15.1	
(42) 3-Fluoro-L-tyrosine	-8.9	
(43) L-Tyrosine	-5.8	

Paper

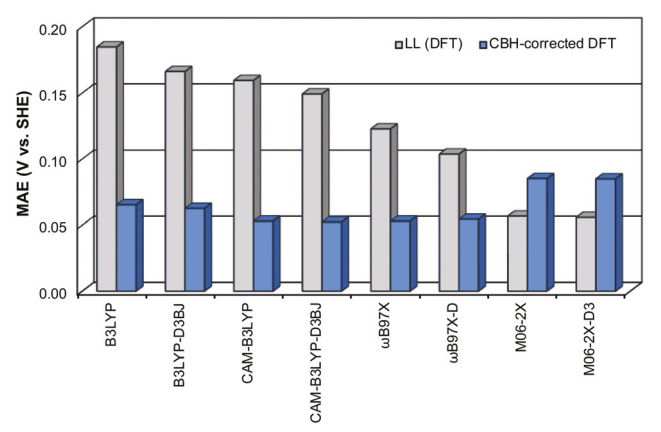
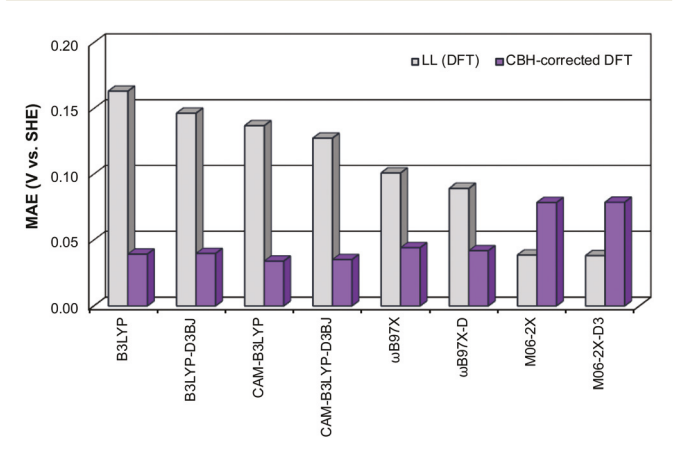


Fig. 8 MAE of LL and CBH-2 redox potentials versus experiment

CAM-B3LYP, CAM-B3LYP-D3BJ, \omegaB97X, and \omegaB97X-D show a marked improvement. Interestingly, while dispersion corrections improve accuracy at the LL, once the CBH correction is applied, functionals that do not include the additional dispersion correction give identical MAEs. After applying the CBH correction, B3LYP achieves a MAE of 0.07 V, and shows the largest error reduction of about 0.12 V. The corrected B3LYP-D3BJ also achieves an increase in accuracy, with a MAE of about 0.06 V compared to its uncorrected MAE of about 0.17 V. CAM-B3LYP, CAM-B3LYP-D3BJ, ω B97X, and ω B97X-D all achieve a MAE of $0.05 \text{ V} (\sim 1.2 \text{ kcal mol}^{-1})$, yielding error reductions between 0.05and 0.11 V. In the case of M06-2X and its dispersion-corrected counterpart, CBH-corrected values actually show a small decrease in accuracy, about 0.03 V. On average, M06-2X, a functional parameterized to reproduce thermochemical data, performs with the same overall accuracy as G4 (0.06 V vs. experiment) for this particular test set. Thus, improving upon this method using G4 fragments is unlikely.

The MAEs of uncorrected and CBH-corrected redox potentials for 43 non-sulfur compounds versus the G4 reference values are shown Fig. 9. Here again, B3LYP shows the largest improvement with an error reduction of 0.12 V. B3LYP, B3LYP-D3BJ, CAM-B3LYP, CAM-B3LYP-D3BJ, ωB97X, and ωB97X-D all achieve MAEs below 0.05 V compared to G4. CAM-B3LYP and its dispersion



MAE of LL and CBH-2 redox potentials versus G4.

corrected counterpart achieve a MAE of 0.03 V (~0.69 kcal mol⁻¹), while ωB97X and ωB97X-D both achieve a MAE of $0.04 \text{ V } (\sim 0.92 \text{ kcal mol}^{-1})$. Nonetheless, M06-2X once again experiences an overall decrease in accuracy of about 0.04 V once the CBH correction is applied. However, although M06-2X errors increase slightly upon applying CBH-Redox, its MAE still hovers around a ~ 2 kcal mol⁻¹ accuracy.

Applying CBH-Redox greatly reduces the range of MAEs across functionals. This is quite impressive, given the confusion that can arise when deciding which functional works best for a given set of conditions. In Fig. 9, MAEs of the LL calculations range from 0.04 to 0.16 V, giving a range of 0.12 V. By contrast, after the CBH correction is applied, the range of MAEs decreases to about 0.05 across functionals. If the M06-2X are not included, the range of MAEs drops to 0.01 V. When experimental values are used as a reference, the range of MAEs across functionals shows a further decrease from 0.13 to 0.04 V. Again, if the Minnesota functionals are not taken into account, the range of MAEs across functionals likewise drops to 0.01 V. The CBH-Redox protocol seeks to eliminate systematic errors by matching bond types in parent and fragment molecules. By doing such, CBH levels the playing field of functional performance, and thus, the choice of functional becomes less important. Given the slew of functionals available for quantum chemical calculations, leveling functional performance alleviates the confusion and complications involved in picking a proper functional.

Fig. 10 shows the overall improvement in MAE due to the application of CBH for each functional group and for each functional tested, corresponding to the 43 molecules in Table 2. Overall, the CBH-Redox protocol produces a significant decrease in error for all functional groups, with a particular improvement seen in amines and methoxybenzenes. Importantly, the largest decrease in performance for the M06-2X functional after the application of the CBH correction is seen in phenols and methoxybenzenes. Coincidentally, these molecules make up the majority of the test set. This could be one contributing factor to the overall reported decrease in performance of the M06-2X functional using the CBH-Redox protocol.

In Table 2, the redox potentials of all 43 non-sulfur molecules in aqueous solvent for both LL uncorrected and CBH-corrected calculations are listed. Also given in the table are experimental and G4 reference values. The structures required to compute LL and CBH-corrected redox potentials reported in Table 2 were optimized with B3LYP/6-31G(2df,p), and all single point calculations were performed at the CAM-B3LYP-D3BJ/6-311++G(3df,2p) level of theory. For the vast majority of potentials listed, the application of CBH-Redox makes a substantial improvement. In most cases, errors are more than halved. However, there are some cases that showed a decrease in accuracy when compared to either experiment, G4, or both. In the case of molecules 20 and 24, adding the CBH correction improves errors relative to G4 but not to experiment. This result is likely attributed to the discrepancy between experimental and G4 reference values. On the other hand, increased errors relative to G4 are typically found when ΔG for the full HL system is not accurately modelled by ΔG of the fragment sums. Employing a CBH-3 fragmentation

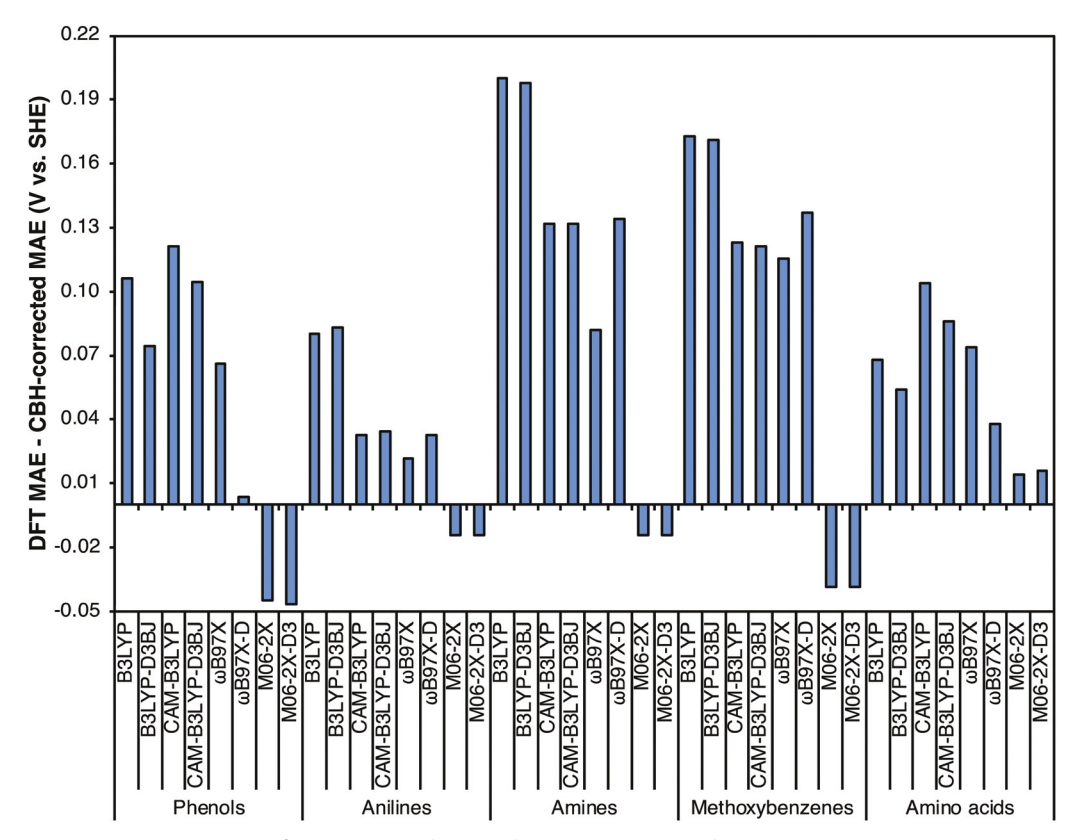


Fig. 10 Overall improvement in MAE due to CBH correction for each functional group and functional tested, compared with experiment. A positive value indicates overall improvement

scheme could perhaps allay this error. Larger fragments capture more of the bonding environment, thus giving a more appropriate correction. Moreover, the effects of ortho substituents and electron delocalization may be better captured at the fragment level. However, if this strategy is employed, care must be taken to ensure that the dihedral angles of the fragments do not deviate far from planarity, making sure to match the planarity of the benzene ring in the parent molecule. Nonetheless, considering overall performance, the MAEs for six out of eight functionals is substantially reduced, with CAM-B3LYP-D3BJ falling from 0.15 to 0.05 V relative to experiment, and from 0.13 to 0.03 V relative to G4.

Table 3 shows the data collected for several sulfur-containing compounds in water. The structures required for the LL and CBH redox potentials reported in Table 3 were optimized with B3LYP/6-31G(2df,p), and all single point calculations reported were performed at the CAM-B3LYP-D3BJ/6-311++G(3df,2p) level of theory. In water, the redox reactions of sulfide compounds are often irreversible due to the chemical instability of the radical site.⁶⁸ In water, thiols are oxidized and subsequently deprotonated, resulting in the formation of a disulfide bond, while thioethers are readily oxidized to sulfoxide and sulfone products. 68,75-77 Moreover, thioethers often adsorb to the surface of the electrode, affecting the accuracy of the experimental measurement.⁷⁶ As shown in Table 3, DFT has a MAE of 0.13 V compared to experiment. The CBH-corrected potentials display a larger error of 0.21 V versus experiment. Experimental values in

water were reported versus the Fc/Fc⁺ couple. Values relative to SHE were obtained by adding the conversion factor of 0.624 V as reported in the literature.³⁸ In aqueous solution, the neutral and radical compounds with functional groups containing N, O and S atoms are stabilized through hydrogen bonding with explicit water molecules in the first solvation shell. However, it has been suggested that SMD does not systematically treat this interaction for thiols.⁷⁸ Likewise, a similar effect is perhaps not captured for thioethers by the solvation model, and thus results in higher redox potentials compared to experiment. Moreover, calculations involving sulfur-containing molecules using the SMD model have been shown to give decreased accuracy when compared with C, H, N, and O species, a result which is consistent with our findings. 43,79,80 Interestingly, when compared with full HL calculated redox potentials, the CBH-corrected values show an improvement over DFT. Indeed, when compared to G4, error decreases from 0.14 V to 0.03 V after applying the CBH correction. As a possible explanation, it may be that neither the low level nor the high level fully captures the effects of solvation; thus, applying the CBH correction yields improved accuracy relative to G4. Additionally, because thioethers typically produce an irreversible potential due to their fast oxidation in water, the errors in experimental reference values may result in deviations when compared with G4 calculations.

As a comparison, redox potential calculations of sulfurcontaining compounds are also given in acetonitrile and compared to experiments that use acetonitrile as a solvent and

Table 2 Redox potentials of 43 organic molecules in aqueous solvent in V vs. SHE. Experimental and G4 values are given, as well as LL and CBH-corrected values. All structures were optimized with B3LYP/6-31G(2df,p), and single point energies were obtained at the CAM-B3LYP-D3BJ/6-311++G(3df,2p) level of theory

	Exp.	G4	DFT	CBH	DFT-Exp.	СВН-Ехр.	DFT-G4	CBH-G
(1) 2,6-Dimethoxyphenol	0.66 ^a	0.63	0.51	0.66	-0.15	0.00	-0.12	0.03
(2) 2-Methoxy-4-formylphenol	0.92^{a}	0.90	0.80	0.95	-0.12	0.03	-0.10	0.05
3) 2-Methoxyphenol	0.79^{a}	0.85	0.70	0.84	-0.09	0.05	-0.15	-0.01
4) 3-Hydroxy-acetophenone	1.09^{a}	1.07	0.93	1.07	-0.15	-0.01	-0.14	0.00
5) 3-Methoxyphenol	1.00^{a}	1.05	0.91	1.06	-0.09	0.06	-0.14	0.01
6) 4-Ethyl-2-methoxyphenol	0.72^{a}	0.72	0.59	0.74	-0.13	0.02	-0.13	0.02
7) 4-Ethylphenol	0.92^{a}	0.92	0.76	0.91	-0.16	-0.01	-0.16	-0.01
8) 4-Hydroxy-acetophenone	1.14^a	1.09	0.99	1.14	-0.15	0.00	-0.10	0.05
9) 4-Methoxyphenol	0.76^{a}	0.77	0.60	0.75	-0.16	-0.01	-0.17	-0.02
10) Bisphenol-A	0.91^{a}	0.82	0.75	0.90	-0.16	-0.01	-0.07	0.08
11) Triclosan	1.01^a	0.93	0.85	1.00	-0.16	-0.01	-0.08	0.07
12) 3-Chlorophenol	1.11^{a}	1.12	0.95	1.10	-0.16	-0.01	-0.17	-0.02
13) 2,4,6-Trichlorophenol	0.93^{a}	0.98	0.82	0.96	-0.11	0.03	-0.16	-0.02
14) 2,4-Dinitrophenol	1.49^{a}	1.43	1.44	1.58	-0.05	0.09	0.01	0.15
15) 2,5-Dimethylphenol	0.86^{a}	0.90	0.75	0.90	-0.11	0.04	-0.15	0.00
16) 2-Chlorophenol	1.05^{a}	1.02	0.85	1.00	-0.20	-0.05	-0.17	-0.02
17) 2-Phenylphenol	0.91^{a}	0.99	0.81	0.96	-0.10	0.05	-0.18	-0.03
18) 4-Nitrophenol	1.25^{a}	1.23	1.14	1.29	-0.11	0.04	-0.09	0.06
19) 4-Cyanophenol	1.21^{a}	1.18	1.05	1.20	-0.16	-0.01	-0.13	0.02
20) 2-Methoxy-5-nitroaniline	1.10^{a}	1.22	1.11	1.24	0.01	0.14	-0.11	0.02
21) 2-Methoxyaniline	0.89^{a}	0.89	0.73	0.86	-0.16	-0.03	-0.16	-0.03
22) 3-Methoxyaniline	1.02^{a}	1.08	0.95	1.08	-0.07	0.06	-0.13	0.00
23) 4-Methoxyaniline	0.77^{a}	0.74	0.57	0.70	-0.20	-0.07	-0.17	-0.04
24) 2-Chloroaniline	1.20^{a}	1.29	1.15	1.28	-0.05	0.08	-0.14	-0.01
25) 4-Chloroaniline	1.06^{a}	1.13	0.99	1.12	-0.07	0.06	-0.14	-0.01
26) 4-Methylaniline	0.93^{a}	0.93	0.77	0.89	-0.16	-0.04	-0.16	-0.04
27) Diethylamine	1.36^{b}	1.19	1.03	1.20	-0.33	-0.16	-0.16	0.01
28) Piperidine	1.34^{b}	1.21	1.09	1.27	-0.25	-0.07	-0.12	0.06
29) Pyrrolidine	1.26^{b}	1.16	0.99	1.16	-0.27	-0.10	-0.17	0.00
(30) Diphenylamine	1.00^{c}	1.07	0.92	1.10	-0.08	0.10	-0.15	0.03
31) <i>n</i> -Methylaniline	0.95^{b}	0.92	0.78	0.94	-0.17	-0.01	-0.14	0.02
32) 1,2,3-Trimethoxybenzene	1.42^{d}	1.41	1.26	1.43	-0.16	0.01	-0.15	0.02
33) 1,2,4-Trimethoxybenzene	1.13^{d}	1.06	0.94	1.10	-0.19	-0.03	-0.12	0.04
34) 1,2-Dimethoxybenzene	1.44^{d}	1.39	1.24	1.41	-0.20	-0.03	-0.15	0.02
35) 1,3-Dimethoxybenzene	1.60^{d}	1.56	1.44	1.60	-0.16	0.00	-0.12	0.04
36) 1,4-Dimethoxybenzene	1.30^{d}	1.21	1.08	1.25	-0.22	-0.05	-0.13	0.04
37) 3-(2-Methoxy-phenoxyl)-1,2-propanediol	1.40^{d}	1.31	1.23	1.39	-0.17	-0.01	-0.08	0.04
38) Anisole	1.62^{d}	1.75	1.60	1.76	-0.02	0.14	-0.15	0.01
39) 3-Amino-L-tyrosine	0.64^{e}	0.45	0.32	0.47	-0.32	-0.17	-0.13	0.02
40) 3-Methoxy-L-tyrosine	0.87^{e}	0.45	0.58	0.72	-0.32 -0.29	-0.17 -0.15	-0.13 -0.08	0.02
41) 3-Nitro-L-tyrosine	1.04^{e}	1.04	1.04	1.19	0.00	0.15	0.00	0.15
42) 3-Fluoro-L-tyrosine	0.90^{e}	0.84	0.74	0.89	-0.16	-0.01	-0.10	0.15
(42) 3 Fidoro E tyrosine (43) L-Tyrosine	0.94^{e}	0.85	0.75	0.89	-0.19	-0.05	-0.10	0.04
MAE					0.15	0.05	0.13	0.03
RMSE ^a Ref. 67. ^b Ref. 66. ^c Ref. 10 and 27. ^d Ref. 65.						0.07	0.13	0.05

Table 3 Redox potentials of sulfur-containing molecules in water in V vs. SHE. Experimental and G4 values are given, as well as LL and CBH-corrected values. All structures were optimized with B3LYP/6-31G(2df,p), and single point energies were obtained at the CAM-B3LYP-D3BJ/6-311++G(3df,2p) level of theory

	Exp.	G4	DFT	CBH	DFT-Exp.	свн-ехр.	DFT-G4	CBH-G4
(44) Benzyl methyl sulfide (45) 2-Hydroxyethyl benzyl sulfide (46) Thioanisole	1.61^{a} 1.56^{a} 1.53^{a}	1.84 1.81 1.60	1.71 1.72 1.41	1.85 1.87 1.62	0.10 0.16 -0.12	0.24 0.31 0.09	-0.13 -0.09 -0.19	0.01 0.06 0.02
MAE					0.13	0.21	0.14	0.03
^a Ref. 68.								

 Fc/Fc^+ as a reference electrode (+0.624 V νs . SHE). Because the effects of pH need not be considered in aprotic solvents, redox potentials calculated in acetonitrile are used as a baseline for

the assessment of the CBH-Redox protocol on sulfur compounds. The structures required for the LL and CBH redox potentials reported in Table 4 were optimized with B3LYP/6-31G(2df,p),

Table 4 Redox potentials of sulfur-containing molecules in acetonitrile in V vs. SHE. Experimental and G4 values are given, as well as LL and CBHcorrected values. All structures were optimized with B3LYP/6-31G(2df,p), and single point energies were obtained at the CAM-B3LYP-D3BJ/6-311++G(3df,2p) level of theory

	Exp.	G4	DFT	СВН	DFT-Exp.	СВН-Ехр.	DFT-G4	CBH-G4
(44) Benzyl methyl sulfide (45) 2-Hydroxyethyl benzyl sulfide (46) Thioanisole	1.86^{a} 1.98^{a} 1.64^{a}	1.88 1.84 1.63	1.75 1.75 1.44	1.89 1.89 1.65	-0.11 -0.23 -0.20	$0.03 \\ -0.09 \\ 0.01$	-0.13 -0.09 -0.19	-0.01 0.05 0.02
MAE					0.18	0.04	0.14	0.03
^a Ref. 68.								

and all single point calculations reported were performed at the CAM-B3LYP-D3BJ/6-311++G(3df,2p) level of theory. As seen in Table 4, the MAE versus experiment drops from 0.18 to 0.04 V and from 0.14 to 0.03 V versus G4 reference values after the CBH correction is applied. Thus, when using acetonitrile as a solvent, applying the CBH correction improves calculated values relative to experiment and G4.

Conclusions

In summary, the current study presents a computational protocol for accurately predicting the redox potentials of a wide range of organic molecules using effective error cancellation schemes. This protocol, termed CBH-Redox, achieves impressive accuracy with a MAE of 0.05 V or below versus G4 for six of the eight density functionals tested. The protocol achieves an impressive accuracy of 0.05 V versus experiment and a MAE of 0.03 V versus G4 at the CAM-B3LYP-D3BJ/ 6-311++G(3df,2p) level of theory. Considering 46 C, O, N, F, Cl, and S atom-containing molecules, the MAEs of all functionals are within the 0.09 V target accuracy. In aqueous solution, CBH-Redox achieves near G4 accuracy. Moreover, the non-sulfur compounds, the error range across all functionals tested decreases from 0.12 V to about 0.05 V versus G4 and from 0.13 V to 0.04 V versus experiment. For sulfur-containing molecules, the accuracy of the solvation model as well as the reliability of experimental reference potentials must be given careful consideration.

Conflicts of interest

There are no conflicts to declare.

Acknowledgements

The methods used in this project were developed based on the support from the National Science Foundation grant CHE-1665427 at Indiana University. We thank Eric M. Collins for stimulating discussions. Big Red II supercomputing facility at Indiana University was used for most of the calculations in this study.

References

1 A. A. Gorodetsky, L. E. P. Dietrich, P. E. Lee, B. Demple, D. K. Newman and J. K. Barton, DNA binding shifts the

- redox potential of the transcription factor SoxR, Proc. Natl. Acad. Sci. U. S. A., 2008, 105, 3684-3689.
- 2 S. Steenken, J. P. Telo, H. M. Novais and L. P. Candeias, One-electron-reduction potentials of pyrimidine-bases, nucleosides, and nucleotides in aqueous-solution - consequences for DNA redox chemistry, J. Am. Chem. Soc., 1992, 114, 4701-4709.
- 3 G. Tell, A. Scaloni, L. Pellizzari, S. Formisano, C. Pucillo and G. Damante, Redox potential controls the structure and DNA binding activity of the paired domain, J. Biol. Chem., 1998, 273, 25062-25072.
- 4 W. Calmano, J. Hong and U. Forstner, Binding and mobilization of heavy-metals in contaminated sediments affected by pH and redox potential, Water Sci. Technol., 1993, 28, 223-235.
- 5 M. B. McBride, Environmental chemistry of soils, Oxford University Press, New York, 1994, p. viii, p. 406.
- 6 T. J. Meyer, Redox pathways applications in catalysis, J. Electrochem. Soc., 1984, 131, C221-C228.
- 7 E. Reisner, V. B. Arion, M. Fatima, C. G. da Silva, R. Lichtenecker, A. Eichinger, B. K. Keppler, V. Y. Kukushkin and A. J. L. Pombeiro, Tuning of redox potentials for the design of ruthenium anticancer drugs - an electrochemical study of [trans-RuCl4L(DMSO)](-) and [trans-RuCl(4)2](-) complexes, where l = imidazole, 1,2,4-triazole, indazole, Inorg. Chem., 2004, 43, 7083-7093.
- 8 R. B. Araujo, A. Banerjee, P. Panigrahi, L. Yang, M. Stromme, M. Sjodin, C. M. Araujo and R. Ahuja, Designing strategies to tune reduction potential of organic molecules for sustainable high capacity battery application, J. Mater. Chem. A, 2017, 5, 4430-4454.
- 9 K. M. Pelzer, L. Cheng and L. A. Curtiss, Effects of functional groups in redox-active organic molecules: A high-throughput screening approach, J. Phys. Chem. C, 2017, 121, 237-245.
- 10 A. V. Marenich, J. M. Ho, M. L. Coote, C. J. Cramer and D. G. Truhlar, Computational electrochemistry: Prediction of liquid-phase reduction potentials, Phys. Chem. Chem. Phys., 2014, 16, 15068-15106.
- 11 L. E. Roy, E. Jakubikova, M. G. Guthrie and E. R. Batista, Calculation of one-electron redox potentials revisited. Is it possible to calculate accurate potentials with density functional methods?, J. Phys. Chem. A, 2009, 113, 6745-6750.
- 12 J. Schüring, H. D. Schulz, W. R. Fischer, J. Böttcher and W. H. Duijnisveld, Redox: Fundamentals, processes and applications, Springer Science & Business Media, 2013.

Paper

13 D. Coskun, S. V. Jerome and R. A. Friesner, Evaluation of the performance of the B3LYP, PBE0, and M06 DFT functionals, and DBLOC-corrected versions, in the calculation of redox potentials and spin splittings for transition metal contain-

ing systems, *J. Chem. Theory Comput.*, 2016, 12, 1121–1128.
14 M. M. Flores-Leonar, R. Moreno-Esparza, V. M. Ugalde-Saldivar and C. Amador-Bedolla, Further insights in DFT calculations of redox potential for iron complexes: The ferrocenium/ferrocene system, *Comput. Theor. Chem.*, 2017, 1099, 167–173.

- 15 J. Baxendale, E. Fielden, C. Capellos, J. Francis, J. Davies, M. Ebert, C. Gilbert, J. Keene, E. Land and A. J. N. Swallow, Pulse radiolysis, *Nature*, 1964, 201, 468–470.
- 16 P. T. Kissinger and W. R. Heineman, Cyclic voltammetry, *J. Chem. Educ.*, 1983, **60**, 702.
- 17 J. B. Conant, The electrochemical formulation of the irreversible reduction and oxidation of organic compounds, *Chem. Rev.*, 1926, 3, 1-40.
- 18 G. Inzelt, A. Lewenstam and F. Scholz, *Handbook of reference electrodes*, Springer, 2013.
- 19 S. J. Konezny, M. D. Doherty, O. R. Luca, R. H. Crabtree, G. L. Soloveichik and V. S. Batista, Reduction of systematic uncertainty in DFT redox potentials of transition-metal complexes, *J. Phys. Chem. C*, 2012, 116, 6349–6356.
- 20 H. Svith, H. Jensen, J. Almstedt, P. Andersson, T. Lundback, K. Daasbjerg and M. Jonsson, On the nature of solvent effects on redox properties, *J. Phys. Chem. A*, 2004, 108, 4805–4811.
- 21 G. E. Zaikov and Z. K. Maizus, Effect of solvents on rates and routes of oxidation reactions, *Adv. Chem. Ser.*, 1968, 150–164.
- 22 M. J. Honeychurch and G. A. Rechnitz, Voltammetry of adsorbed molecules. Part 2: Irreversible redox systems, *Electroanalysis*, 1998, **10**, 453–457.
- 23 M. H. Baik and R. A. Friesner, Computing redox potentials in solution: Density functional theory as a tool for rational design of redox agents, *J. Phys. Chem. A*, 2002, 106, 7407–7412.
- 24 B. T. Psciuk, R. L. Lord, B. H. Munk and H. B. Schlegel, Theoretical determination of one-electron oxidation potentials for nucleic acid bases, *J. Chem. Theory Comput.*, 2012, 8, 5107–5123.
- 25 B. Thapa and H. B. Schlegel, Calculations of pK_a 's and redox potentials of nucleobases with explicit waters and polarizable continuum solvation, *J. Phys. Chem. A*, 2015, **119**, 5134–5144.
- 26 M. Uudsemaa and T. Tamm, Density-functional theory calculations of aqueous redox potentials of fourth-period transition metals, *J. Phys. Chem. A*, 2003, **107**, 9997–10003.
- 27 J. M. Ho, Are thermodynamic cycles necessary for continuum solvent calculation of p K_a 's and reduction potentials?, *Phys. Chem. Chem. Phys.*, 2015, 17, 2859–2868.
- 28 R. J. Bartlett and M. Musial, Coupled-cluster theory in quantum chemistry, *Rev. Mod. Phys.*, 2007, **79**, 291–352.
- 29 L. A. Curtiss, P. C. Redfern and K. Raghavachari, Gaussian-4 theory, J. Chem. Phys., 2007, 126, 084108.
- 30 L. J. Kettle, S. P. Bates and A. R. Mount, Calculations of the electronic structure of substituted indoles and prediction of their oxidation potentials, *Phys. Chem. Chem. Phys.*, 2000, 2, 195–201.

- 31 S. N. Pieniazek, F. R. Clemente and K. N. Houk, Sources of error in DFT computations of C-C bond formation thermochemistries: Pi-> sigma transformations and error cancellation by DFT methods, *Angew. Chem., Int. Ed.*, 2008, 47, 7746–7749.
- 32 E. A. C. Bushnell and R. J. Boyd, Assessment of several DFT functionals in calculation of the reduction potentials for Ni-, Pd-, and Pt-bis-ethylene-1,2-dithiolene and -diselenolene complexes, *J. Phys. Chem. A*, 2015, **119**, 911–918.
- 33 W. J. Hehre, R. Ditchfield, L. Radom and J. A. Pople, Molecular orbital theory of the electronic structure of organic compounds. V. Molecular theory of bond separation, *J. Am. Chem. Soc.*, 1970, **92**, 4796–4801.
- 34 R. O. Ramabhadran and K. Raghavachari, Theoretical thermochemistry for organic molecules: Development of the generalized connectivity-based hierarchy, *J. Chem. Theory Comput.*, 2011, 7, 2094–2103.
- 35 E. M. Collins, A. Sengupta, D. I. AbuSalim and K. Raghavachari, Accurate thermochemistry for organic cations via error cancellation using connectivity-based hierarchy, *J. Phys. Chem. A*, 2018, 122, 1807–1812.
- 36 S. Debnath, A. Sengupta and K. Raghavachari, Eliminating systematic errors in DFT via connectivity-based hierarchy: Accurate bond dissociation energies of biodiesel methyl esters, J. Phys. Chem. A, 2019, 123, 3543–3550.
- 37 B. Thapa and K. Raghavachari, Accurate p*K*_a evaluations for complex bio-organic molecules in aqueous media, *J. Chem. Theory Comput.*, 2019, **15**, 6025–6035.
- 38 J. Ho; M. Coote; C. Cramer and D. Truhlar, Theoretical Calculation of Reduction Potentials, in *Theoretical Calculation* of Reduction Potentials, ed. O. Hammerich and B. Speiser, CRC Press, Taylor and Francis Group, 5th edn, 2015, pp. 229–259.
- 39 R. R. Gagne, C. A. Koval and G. C. Lisensky, Ferrocene as an internal standard for electrochemical measurements, *Inorg. Chem.*, 1980, **19**, 2854–2855.
- 40 M. Namazian, C. Y. Lin and M. L. Coote, Benchmark calculations of absolute reduction potential of ferricinium/ ferrocene couple in nonaqueous solutions, *J. Chem. Theory Comput.*, 2010, 6, 2721–2725.
- 41 J. W. Diggle and A. J. Parker, Liquid junction potentials in electrochemical cells involving a dissimilar solvent junction, *Aust. J. Chem.*, 1974, 27, 1617–1621.
- 42 J. E. Bartmess, Thermodynamics of the electron and the proton, *J. Phys. Chem.*, 1994, **98**, 6420–6424.
- 43 A. V. Marenich, C. J. Cramer and D. G. Truhlar, Universal solvation model based on solute electron density and on a continuum model of the solvent defined by the bulk dielectric constant and atomic surface tensions, *J. Phys. Chem. B*, 2009, **113**, 6378–6396.
- 44 G. Penketh, The oxidation potentials of phenolic and amino antioxidants, *J. Appl. Chem.*, 1957, 7, 512–521.
- 45 J. M. Ho and M. L. Coote, First-principles prediction of acidities in the gas and solution phase, *WIREs Comput. Mol. Sci.*, 2011, **1**, 649–660.
- 46 D. M. Camaioni and C. A. Schwerdtfeger, Comment on "accurate experimental values for the free energies of

PCCP

- hydration of H⁺, OH⁻, and H₃O⁺", J. Phys. Chem. A, 2005, **109**, 10795-10797.
- 47 A. A. Isse and A. Gennaro, Absolute potential of the standard hydrogen electrode and the problem of interconversion of potentials in different solvents, J. Phys. Chem. B, 2010, 114, 7894-7899.
- 48 C. P. Kelly, C. J. Cramer and D. G. Truhlar, Aqueous solvation free energies of ions and ion-water clusters based on an accurate value for the absolute aqueous solvation free energy of the proton, J. Phys. Chem. B, 2006, 110, 16066-16081.
- 49 S. E. Wheeler, K. N. Houk, P. Schleyer and W. D. Allen, A hierarchy of homodesmotic reactions for thermochemistry, J. Am. Chem. Soc., 2009, 131, 2547-2560.
- 50 P. George, M. Trachtman, C. W. Bock and A. M. Brett, An alternative approach to the problem of assessing stabilization energies in cyclic conjugated hydrocarbons, Theor. Chem. Acc., 1975, 38, 121-129.
- 51 M. J. Frisch, G. Trucks, H. Schlegel, G. Scuseria, M. Robb, J. Cheeseman, G. Scalmani, V. Barone, B. Mennucci and G. A. Petersson, Gaussian 16, revision a.-03, Gaussian, Inc., Wallingford, CT, 2016.
- 52 A. D. Becke, Density-functional thermochemistry. I. The effect of the exchange-only gradient correction, J. Chem. Phys., 1992, 96, 2155-2160.
- 53 A. D. Becke, Density-functional thermochemistry. V. Systematic optimization of exchange-correlation functionals, J. Chem. Phys., 1997, 107, 8554-8560.
- 54 J.-D. Chai and M. Head-Gordon, Long-range corrected hybrid density functionals with damped atom-atom dispersion corrections, Phys. Chem. Chem. Phys., 2008, 10, 6615-6620.
- 55 S. Grimme, J. Antony, S. Ehrlich and H. Krieg, A consistent and accurate ab initio parametrization of density functional dispersion correction (DFT-D) for the 94 elements H-Pu, J. Chem. Phys., 2010, 132, 154104.
- 56 S. Grimme, S. Ehrlich and L. Goerigk, Effect of the damping function in dispersion corrected density functional theory, J. Comput. Chem., 2011, 32, 1456-1465.
- 57 C. Lee, W. Yang and R. G. Parr, Development of the Colle-Salvetti correlation-energy formula into a functional of the electron density, Phys. Rev. B: Condens. Matter Mater. Phys., 1988, 37, 785.
- 58 T. Yanai, D. P. Tew and N. C. Handy, A new hybrid exchangecorrelation functional using the coulomb-attenuating method (CAM-B3LYP), Chem. Phys. Lett., 2004, 393, 51-57.
- 59 Y. Zhao and D. G. Truhlar, The M06 suite of density functionals for main group thermochemistry, thermochemical kinetics, noncovalent interactions, excited states, and transition elements: Two new functionals and systematic testing of four M06-class functionals and 12 other functionals, Theor. Chem. Acc., 2008, 120, 215-241.
- 60 M. M. Francl, W. J. Pietro, W. J. Hehre, J. S. Binkley, M. S. Gordon, D. J. DeFrees and J. A. Pople, Self-consistent molecular orbital methods. XXIII. A polarization-type basis set for second-row elements, J. Chem. Phys., 1982, 77, 3654-3665.

- 61 P. C. Hariharan and J. A. Pople, The influence of polarization functions on molecular orbital hydrogenation energies, Theor. Chim. Acta, 1973, 28, 213-222.
- 62 R. Krishnan, J. S. Binkley, R. Seeger and J. A. Pople, Selfconsistent molecular orbital methods. XX. A basis set for correlated wave functions, J. Chem. Phys., 1980, 72, 650-654.
- 63 E. O'Brien, M. E. Holt, M. K. Thompson, L. E. Salay, A. C. Ehlinger, W. J. Chazin and J. K. Barton, The [4Fe4S] cluster of human DNA primase functions as a redox switch using DNA charge transport, Science, 2017, 355, 813-822.
- 64 M. R. Defelippis, C. P. Murthy, F. Broitman, D. Weinraub, M. Faraggi and M. H. Klapper, Electrochemical properties of tyrosine phenoxy and tryptophan indolyl radicals in peptides and amino-acid-analogs, J. Phys. Chem., 1991, 95, 3416-3419.
- 65 M. Jonsson, J. Lind, T. Reitberger, T. E. Eriksen and G. Merenyi, Redox chemistry of substituted benzenes - the one-electron reduction potentials of methoxy-substituted benzene radical cations, J. Phys. Chem., 1993, 97, 11278–11282.
- 66 M. Jonsson, D. D. M. Wayner and J. Lusztyk, Redox and acidity properties of alkyl- and arylamine radical cations and the corresponding aminyl radicals, J. Phys. Chem., 1996, 100, 17539-17543.
- 67 A. S. Pavitt, E. J. Bylaska and P. G. Tratnyek, Oxidation potentials of phenols and anilines: Correlation analysis of electrochemical and theoretical values, Environ. Sci.: Processes Impacts, 2017, 19, 339-349.
- 68 K. Taras-Goslinska and M. Jonsson, Solvent effects on the redox properties of thioethers, J. Phys. Chem. A, 2006, 110, 9513-9517.
- 69 T. A. Enache and A. M. Oliveira-Brett, Boron doped diamond and glassy carbon electrodes comparative study of the oxidation behaviour of cysteine and methionine, Bioelectrochemistry, 2011, 81, 46-52.
- 70 J. Baker, A. Scheiner and J. Andzelm, Spin contamination in density-functional theory, Chem. Phys. Lett., 1993, 216, 380-388.
- 71 A. S. Menon and L. Radom, Consequences of spin contamination in unrestricted calculations on open-shell species: Effect of Hartree-Fock and Moller-Plesset contributions in hybrid and double-hybrid density functional theory approaches, J. Phys. Chem. A, 2008, 112, 13225-13230.
- 72 A. Sengupta and K. Raghavachari, Prediction of accurate thermochemistry of medium and large sized radicals using connectivity-based hierarchy (CBH), J. Chem. Theory Comput., 2014, 10, 4342-4350.
- 73 W. T. Dixon and D. Murphy, Molecular; Physics, C., Determination of the acidity constants of some phenol radical cations by means of electron spin resonance, J. Chem. Soc., Faraday Trans. 2, 1976, 72, 1221-1230.
- 74 J. J. Warren, J. R. Winkler and H. B. Gray, Redox properties of tyrosine and related molecules, FEBS Lett., 2012, 586, 596-602.
- 75 M. N. Elinson and J. Simonet, Electrochemical oxidation of aliphatic sulfides under very weakly nucleophilic conditions the transient formation of a dicationic dimer, J. Electroanal. Chem., 1992, 336, 363-367.
- 76 Sanaullah, G. S. Wilson and R. S. Glass, The effect of pH and complexation of amino-acid functionality on the redox chemistry

Paper

of methionine and X-ray structure of [Co(En)(2)(L-Met)](ClO₄)(2).

H₂O, J. Inorg. Biochem., 1994, 55, 87-99.

- 77 M. Schmidt am Busch and E. W. Knapp, One-electron reduction potential for oxygen- and sulfur-centered organic radicals in protic and aprotic solvents, *J. Am. Chem. Soc.*, 2005, **127**, 15730–15737.
- 78 B. Thapa and H. B. Schlegel, Density functional theory calculation of pK_a 's of thiols in aqueous solution using explicit water molecules and the polarizable continuum model, *J. Phys. Chem. A*, 2016, **120**, 5726–5735.
- 79 P. Lian, R. C. Johnston, J. M. Parks and J. C. Smith, Quantum chemical calculation of pKas of environmentally relevant functional groups: Carboxylic acids, amines, and thiols in aqueous solution, *J. Phys. Chem. A*, 2018, **122**, 4366–4374.
- 80 L. Xu and M. L. Coote, Methods to improve the calculations of solvation model density solvation free energies and associated aqueous pK_a values: Comparison between choosing an optimal theoretical level, solute cavity scaling, and using explicit solvent molecules, *J. Phys. Chem. A*, 2019, 123, 7430–7438.